Appl. Set-Valued Anal. Optim. 8 (2026), No. 3, pp. 357-372
Available online at http://asvao.biemdas.com
https://doi.org/10.23952/asvao.8.2026.3.05

AN ENHANCED PRP CONJUGATE GRADIENT METHOD BY ADAPTING A NEW LINE SEARCH FOR UNCONSTRAINED OPTIMIZATION AND IMAGE RESTORATION PROBLEMS

RAOUF ZIADI[1,*], ASMA MAIZA[1], ABD ELHAMID MEHAMDIA[2], MOHAMMED A. SALEH[3]

[1]*Laboratory of Fundamental and Numerical Mathematics (LMFN), Department of Mathematics, University Setif - 1 - Ferhat Abbas, Algeria*
[2]*Laboratory Informatics and Mathematics (LIM), University M'Hamed BOUGARA Boumerdès, Algeria*
[3]*Department of Cybersecurity, College of Computer, Qassim University, Saudi Arabia*

Abstract. Conjugate gradient methods are considered among the most efficient methods for solving large-scale optimization problems. Among them, the PRP variant has attracted the attention due to its straightforward iterative process and low memory requirements. In this paper, a new inexact line search method is proposed and the existence of a steplength that meets the new line search conditions is obtained. The generated descent direction and the convergence properties of the PRP method are studied under the new line search conditions, where the global convergence is proven under mild assumptions.
Keywords. Image restoration; Inexact line search; Global convergence; Polak-Ribière-Polyak conjugate gradient method; Unconstrained optimization.
2020 Mathematics Subject Classification. 90C26, 90C53, 90C30.

1. INTRODUCTION

We consider in this work the following unconstrained optimization problem:

$$f^* = \min_{x\in\mathbb{R}^n} f(x), \tag{P}$$

where $f:\mathbb{R}^n \to \mathbb{R}$ is continuously differentiable with gradient $g(x) = \nabla f(x)$. Numerous problems in real-word applications can be expressed as unconstrained optimization problems that involve differentiable cost functions [29]. Finding solutions for these problems becomes difficult as their dimensions are high. Various techniques, such as Newton's method, quasi-Newton methods, and conjugate gradient (CG) methods, were explored to find the most efficient way. CG method is a popular approach due to their straightforward iterative process and low memory requirements. They are widely employed in numerous applications; see, e.g., [2, 6, 11, 14, 15, 28]. Starting from a point $x_0 \in \mathbb{R}^n$, the sequence of points $\{x_k\}_{k\in\mathbb{N}} \subset \mathbb{R}^n$ is generated by the following recursive scheme:

$$x_{k+1} = x_k + \alpha_k d_k, \quad k \in \mathbb{N}, \tag{1.1}$$

[*]Corresponding author.
E-mail address: ziadi.raouf@gmail.com; raouf.ziadi@univ-setif.dz (R. Ziadi).
Received 6 August 2025; Accepted 14 January 2026; Published online 15 September 2026.
©2026 Applied Set-Valued Analysis and Optimization

where d_k is the descent direction and α_k is the steplength that ensures that $f(x_{k+1}) \leq f(x_k)$. The determination of the steplength α_k is crucial for global convergence. Usually, it is determined using inexact line searches, which guarantee taking steps that should be neither too long nor too short, such as the weak Wolfe line search

$$f(x_k+\alpha_k d_k)-f(x_k) \leq \alpha_k \delta d_k^t g_k,\ g(x_k+\alpha_k d_k)^t d_k \geq \sigma d_k^t g_k,$$

or the strong Wolfe line search

$$f(x_k+\alpha_k d_k)-f(x_k) \leq \alpha_k \delta d_k^t g_k,\ \left|g(x_k+\alpha_k d_k)^t d_k\right| \leq -\sigma d_k^t g_k,$$

where $0<\delta<\sigma<1$. The descent search direction d_k is typically computed by the following iterative formula

$$d_0=-g_0;\ d_{k+1}=-g_{k+1}+\beta_k d_k, \quad k \in \mathbb{N}^*,$$

where $\beta_k \in \mathbb{R}$ is the conjugate parameter that characterizes the various conjugate gradient variants. The most famous classical conjugate gradient methods include HS (Hestenes and Stiefel) [12], FR (Fletcher and Reeves) [8], PRP (Polak-Ribière-Polyak) [17, 18], CD (conjugate descent) [8], LS (Liu and Storey) [13], and DY (Dai and Yuan) [5], where their parameters β_k are given respectively as follows

$$\beta_k^{HS}=\frac{g_{k+1}^t y_k}{d_k^t y_k}, \beta_k^{PRP}=\frac{g_{k+1}^t y_k}{\|g_k\|^2}, \beta_k^{LS}=-\frac{g_{k+1}^t y_k}{g_k^t d_k}$$

$$\beta_k^{FR}=\frac{\|g_{k+1}\|^2}{\|g_k\|^2}, \beta_k^{CD}=-\frac{\|g_{k+1}\|^2}{g_k^t d_k}, \beta_k^{DY}=\frac{\|g_{k+1}\|^2}{d_k^t y_k},$$

where $y_k=g_{k+1}-g_k$ and $\|.\|$ denotes the Euclidean norm in $\mathbb{R}^n$. The DY, CD and FR methods have better theoretical convergence properties, but practically, they are less effective. Conversely, the LS, HS and PRP methods are more efficient in practice, but they may not always be convergent. Over the last decade, this research topic has attracted attention and numerous studies have developed efficient conjugate gradient formulas with good numerical performance and convergence properties. For more recent conjugate gradient methods, we refer to [3, 19, 20, 23]. Although the PRP method is considered classical, it remains competitive and robust for solving large-scale complex problems. Despite its practical success, global convergence is uncertain for non-convex minimization. Numerous studies discussed this drawback. Powell [16] proved the divergence of the PRP method for non-convex minimization by giving a counterexample. Moreover, Dai [4] proved that the PRP method may generate ascent directions during the searching process. To address these shortcomings, Gilbert and Nocedal [10] proposed a modified PRP formula, known as the PRP$^+$ method, in which the parameter $\beta_k^{\mathrm{PRP}^+}$ is nonnegative:

$$\beta_k^{\mathrm{PRP}^+}=\max\{0, \beta_k^{\mathrm{PRP}}\}.$$

In recent years, several modifications of β_k^{PRP} were developed to ameliorate the performance of the PRP method. Wei et al. [21] introduced a modification of β_k^{PRP}, defined by

$$\beta_k^{WYL}=\frac{g_k^T\left(g_k-\frac{\|g_k\|}{\|g_{k-1}\|}g_{k-1}\right)}{\|g_{k-1}\|^2}.$$

The WYL method is competitive and converges globally under the strong Wolfe line search.

More recently, Yousif et al. [22] proposed another modification of the PRP method, termed OPRP, in which the parameter β_k^{PRP} is restricted to $\left(-\mu\frac{\|\mathbf{g}_k\|^2}{\|\mathbf{d}_{k-1}\|^2}, \mu\frac{\|\mathbf{g}_k\|^2}{\|\mathbf{d}_{k-1}\|^2}\right)$, in which the corresponding coefficient β_k^{OPRP} is defined as

$$\beta_k^{\text{OPRP}} = \begin{cases} \beta_k^{\text{PRP}} & \text{if } -\mu\dfrac{\|g_k\|^2}{\|d_{k-1}\|^2} < \beta_k^{\text{PRP}} < \mu\dfrac{\|g_k\|^2}{\|d_{k-1}\|^2}, \\ 0 & \text{otherwise,} \end{cases}$$

where $\mu > 2$ is a given constant. This modification is computationally competitive and guarantees global convergence under the strong Wolfe conditions.

Motivated by this idea, Yousif et al. [23] further proposed a new PRP-type method by combining $\beta_k^{\text{PRP}^+}$ and β_k^{OPRP} whose parameter is defined as

$$\beta_k = \begin{cases} \beta_k^{\text{PRP}} & \text{if } \beta_k^{\text{PRP}} > -\mu\frac{\|\mathbf{g}_k\|^2}{\|\mathbf{d}_{k-1}\|^2} \\ 0 & \text{otherwise,} \end{cases}$$

where $\mu > 2$.

Efforts to improve the performance of the PRP algorithm through modifications of its β_k parameter have been made. Numerous studies focused on enhancing its efficiency and ensuring global convergence by proposing new line search strategies. Zhou and Li [27] proved the global convergence of the PRP method by using a modified Armijo line search technique, and their proposed method exhibits good performance. The convergence of the PRP method under several inexact line search techniques was analyzed in [24, 25]. Recently, Yuan et al. [26] studied the convergence of the PRP method via a steplength α_k that meets the following conditions:

$$f(x_k + \alpha_k d_k) - f(x_k) \leq \alpha_k \delta d_k^t g_k + \delta \frac{\alpha_k^2}{2}\|d_k\|^2 \delta_1,$$
$$g(x_k + \alpha_k d_k)^t d_k \geq \sigma d_k^t g_k + \delta \alpha_k \|d_k\|^2 \delta_1,$$

where $\delta \in (0, \frac{1}{2})$, $\sigma \in (\delta, 1)$ and δ_1 is a sufficiently small scalar. Their proposed modification is competitive, and the generated search directions satisfy the sufficient descent condition.

In order to combine good practical performance and powerful convergence properties, we adopt a new inexact line search technique that fits in with the PRP conjugate gradient parameter and can also be useful for other gradient descent methods. The proposed approach, named PRP-NLS (PRP with New Line Search), converges globally under mild assumptions. The algorithm is successfully applied on a broad set of test functions (with varied analytical expressions and structures) that ranges from the simplest to the hardest, as well as image processing.

2. The New Line Search Technique and the Algorithm

We adopt a new inexact line search technique that fits in with the PRP parameter where α_k satisfies the following conditions:

$$f(x_k + \alpha_k d_k) - f(x_k) \leq \alpha_k \delta d_k^t g_k \frac{\|g_k\|^2}{\|d_k\|^2}, \tag{2.1}$$

$$\left|g(x_k + \alpha_k d_k)^t d_k\right| \leq -\sigma d_k^t g_k \frac{\|g_k\|^2}{\|d_k\|^2}, \tag{2.2}$$

where $\sigma \in \left(0, \frac{\mu-1}{1.2\mu^2}\right]$, with $1 < \mu < 2$ and $0 < \delta < \sigma$. Since $1 < \mu < 2$, it follows that $0 < \delta < \sigma < 1$. The new line search technique is a modification of the strong Wolfe one by adding the term $\frac{\|g_k\|^2}{\|d_k\|^2}$ (to the right side of the strong Wolfe inequalities). The new term depends on the gradient values and the descent direction at each point x_k. We adopt this line search to fit in with the PRP parameter and ensure global convergence with good numerical performance. This modification permits getting a steplength that is neither too long nor too short. As demonstrated below, the proposed method exhibits good convergence properties and satisfactory performance. The main steps of the PRP-NLS method are sketched in Algorithm 2.1 below.

Algorithm 2.1 The PRP-NLS algorithm

Step 0: (Initialization) Choose the parameters μ, δ and σ such that $0 < \delta < \sigma < \frac{\mu-1}{1.2\mu^2}$, with $1 < \mu < 2$. Choose a scalar $\varepsilon > 0$ sufficiently small to stop the algorithm. Select a point $x_0 \in \mathbb{R}^n$, and compute $f(x_0)$. Set $g_0 = \nabla f(x_0)$, $d_0 = -g_0$, and put $k = 0$.
Step 1: If $\|g_k\| \leq \varepsilon$, then stop; otherwise go to the next step.
Step 2: Compute the steplength α_k using the new line search technique (2.1) and (2.2).
Step 3: Put $x_{k+1} = x_k + \alpha_k d_k$ and set $g_{k+1} = \nabla f(x_{k+1})$.
Step 4: **Search direction computation:** if the restart criterion of Powell $|g_{k+1}^t g_k| \geq 0.2\,\|g_{k+1}\|^2$ holds, then set $d_{k+1} = -g_{k+1}$; otherwise set $d_{k+1} = -g_{k+1} + \beta_k^{PRP} d_k$.
Step 5: Set $k = k+1$ and go back to Step 1.

3. The Sufficient Descent Property

We first prove the following result that is needed later.

Theorem 3.1. *Let $\{g_k\}_{k\in\mathbb{N}}$, $\{\beta_k\}_{k\in\mathbb{N}}$ and $\{d_k\}_{k\in\mathbb{N}}$ be the sequences generated by the PRP-NLS Algorithm under conditions (2.1) and (2.2). Then*

$$\|g_k\|/\|d_k\| \leq \mu, \forall k \in \mathbb{N}. \tag{3.1}$$

Proof. If the Powell condition holds, then $\left|g_k^t g_{k+1}\right| \geq 0.2\|g_{k+1}\|^2$. The search direction d_k is given by $d_k = -g_k$, and relation (3.1) holds. Now, if Powell condition does not hold. We prove the above relation by recurrence. For $k = 0$, condition (3.1) holds, due to $d_0 = -g_0$. Assume that relation (3.1) satisfied for $k \geq 1$. One next proves it for $k+1$. For $k+1$, one has

$$d_{k+1} = -g_{k+1} + \beta_k^{PRP} d_k, \tag{3.2}$$

Multiplying both sides of (3.2) by g_{k+1}^t, we have $d_{k+1}^t g_{k+1} = -\|g_{k+1}\|^2 + \beta_k^{PRP} d_k^t g_{k+1}$. On the other hand, we have

$$\left|\beta_k^{PRP}\right| = \frac{\left|\|g_{k+1}\|^2 - g_{k+1}^t g_k\right|}{\|g_k\|^2} \leq \frac{\|g_{k+1}\|^2 + \left|g_{k+1}^t g_k\right|}{\|g_k\|^2} \leq 1.2\frac{\|g_{k+1}\|^2}{\|g_k\|^2}. \tag{3.3}$$

Hence, it follows from condition (2.2) that

$$\begin{aligned} \|g_{k+1}\|^2 &\le \left|d_{k+1}^t g_{k+1}\right| - \sigma\left|\beta_k^{PRP}\right| d_k^t g_k \frac{\|g_k\|^2}{\|d_k\|^2} \\ &\le \left|d_{k+1}^t g_{k+1}\right| + \sigma\left|\beta_k^{PRP}\right| \left|d_k^t g_k\right| \frac{\|g_k\|^2}{\|d_k\|^2} \\ &\le \|d_{k+1}\|\,\|g_{k+1}\| + \sigma\left|\beta_k^{PRP}\right| \frac{\|g_k\|^3}{\|d_k\|} \\ &\le \|d_{k+1}\|\,\|g_{k+1}\| + 1.2\sigma\frac{\|g_k\|}{\|d_k\|}\,\|g_{k+1}\|^2. \end{aligned} \tag{3.4}$$

Note that

$$\left(1 - 1.2\sigma\frac{\|g_k\|}{\|d_k\|}\right) \ge (1 - 1.2\sigma\mu) \ge (1 - \frac{\mu-1}{\mu}) = \frac{1}{\mu} > 0. \tag{3.5}$$

Dividing both sides of (3.4) by $\|g_{k+1}\|\,.\,\|d_{k+1}\|$, we see from (3.5) that

$$\frac{\|g_{k+1}\|}{\|d_{k+1}\|} \le \frac{1}{\left(1 - 1.2\sigma\frac{\|g_k\|}{\|d_k\|}\right)} = \mu.$$

Thus, the proof is complete □

Now, we are in the position to prove the sufficient descent condition.

Theorem 3.2. *The sequences $\{g_k\}_{k\in\mathbb{N}}$, $\{\beta_k\}_{k\in\mathbb{N}}$ and $\{d_k\}_{k\in\mathbb{N}}$ generated by the PRP-NLS Algorithm under the new line search conditions (2.1) and (2.2) with $\sigma \in \left(0, \frac{\mu-1}{1.2\mu^2}\right]$ and $1 < \mu < 2$ satisfy*

$$g_k^t d_k \leqslant -\xi\,\|g_k\|^2,\ \forall k \in \mathbb{N} \tag{3.6}$$

where $\xi > 0$.

Proof. It is evident that, in the case where the restart criterion of Powell holds, i.e, $\left|g_k^t g_{k+1}\right| \ge 0.2\|g_{k+1}\|^2$, $d_k = -g_k$ and relation (3.6) holds. If the Powell condition does not hold, we prove the above relation by induction. For $k = 0$, $d_0 = -g_0$, which implies that $d_0^t g_0 = -\|g_0\|^2$, and relation (3.6) holds. Suppose that (3.6) is true for $k \ge 1$. For $k+1$, by multiplying both sides of (3.2) by g_{k+1}^t, we obtain

$$\begin{aligned} d_{k+1}^t g_{k+1} &\le -\|g_{k+1}\|^2 + \left|\beta^{PRP}\right| \left|d_k^t g_{k+1}\right| \\ &\le -\|g_{k+1}\|^2 + 1.2\sigma\frac{\|g_{k+1}\|^2}{\|g_k\|^2}\|g_k\|\|d_k\|\frac{\|g_k\|^2}{\|d_k\|^2} \text{ (using (2.2) and (3.4))} \\ &\le -\|g_{k+1}\|^2 + 1.2\sigma\frac{\|g_k\|}{\|d_k\|}\,\|g_{k+1}\|^2 \\ &\le -\|g_{k+1}\|^2(1 - 1.2\sigma\mu)) \le -\frac{1}{\mu}\,\|g_{k+1}\|^2 \text{ (using (3.1) and (3.5)).} \end{aligned}$$

Then the proof completes for $\xi = \frac{1}{\mu}$. □

4. The Convergence Analysis

Before analysing the convergence of the proposed approach, we first show that it is well-defined. In the next theorem, we prove the existence of a steplength α ($0 < \alpha < \infty$) that meets conditions (2.1) and (2.2), where $0 < \delta < \sigma$, with $\sigma \in (0, \frac{\mu-1}{1.2\mu^2}]$ and $1 < \mu < 2$.

Theorem 4.1. *Let f be a twice continuously differentiable function that is bounded below. If $g_k^t d_k < 0$, then there exists a strictly positive real value α that meets conditions (2.1) and (2.2).*

Proof. Define the function $h(\alpha) = f(x_k + \alpha d_k) - f(x_k) - \delta \alpha g_k^t d_k \frac{\|g_k\|^2}{\|d_k\|^2}$. Using a standard Taylor development, it follows from relation (3.1) that

$$h(\alpha) = \alpha g_k^t d_k - \delta \alpha g_k^t d_k \frac{\|g_k\|^2}{\|d_k\|^2} + o(\alpha) \leq \alpha \left(1 - \frac{\mu - 1}{1.2}\right) g_k^t d_k + o(\alpha) < 0.$$

Since f is bounded below, it results that $\lim_{\alpha \to +\infty} h(\alpha) = +\infty$ and $h(0) = 0$. Hence, $h(.)$ changes its sign, and then there exists a constant $\tau > 0$ such that $h(\tau) = 0$. It is clear that $h(\alpha)$ has a negative sign over the interval $[0, \tau]$, and its global minimum can not occur at the endpoints, due to $h(0) = h(\tau) = 0$. Therefore, the exists $\alpha^* \in (0, \tau)$, such that $h(\alpha^*) < 0$ and $h'(\alpha^*) = 0$. Hence $h(\alpha^*) = f(x_k + \alpha^* d_k) - f(x_k) - \delta \alpha^* g_k^t d_k \frac{\|g_k\|^2}{\|d_k\|^2} < 0$, so that

$$f(x_k + \alpha^* d_k) < f(x) + \delta \alpha^* g_k^t d_k \frac{\|g_k\|^2}{\|d_k\|^2},$$

and the first condition (2.1) holds. On the other hand, we have $h'(\alpha) = g_{k+1}^t d_k - \delta g_k^t d_k \frac{\|g_k\|^2}{\|d_k\|^2}$. Since $h'(\alpha^*) = 0$, then

$$\sigma g_k^t d_k \frac{\|g_k\|^2}{\|d_k\|^2} \leq \delta g_k^t d_k \frac{\|g_k\|^2}{\|d_k\|^2} = g_{k+1}^t d_k < 0.$$

Thus

$$\left|g_{k+1}^t d_k\right| \leq -\sigma g_k^t d_k \frac{\|g_k\|^2}{\|d_k\|^2}.$$

Thus (2.2) is also satisfied. $\square$

4.1. The global convergence.

The global convergence is crucial for any conjugate gradient method. To investigate it, we need the following assumptions.

Assumption 4.1. The level set $\Omega = \{x \in \mathbb{R}^n | \ f\ (x) \leq f\ (x_0)\}$ is bounded for any starting point x_0.

Assumption 4.2. f is continuously differentiable whose gradient function g satisfies the Lipschitz condition in some closed neighbourhood $\mathcal{N}$ of Ω, that is, there exists $L > 0$ such that $\|g(x) - g(y)\| \leq L\|x - y\|\|$ for all $x, y \in \mathcal{N}$.

The above assumptions imply the existence of a real number $\Gamma \geq 0$ such that $\|g_k\| \leq \Gamma$ for all x in Ω. To see the global convergence of the PRP-NLS algorithm (see Theorem 4.2 below), we need to prove the following results.

Lemma 4.1. *Consider the sequences* $\{g_k\}_{k\in\mathbb{N}}$, $\{\alpha_k\}_{k\in\mathbb{N}}$ *and* $\{d_k\}_{k\in\mathbb{N}}$ *generated by the PRP-NLS algorithm; then, for some* $\varpi > 0$, $g_k^t d_k \geq -\varpi \|g_k\|^2$.

Proof. By multiplying Equation (3.2) by g_{k+1}, we have $|d_{k+1}^t g_{k+1}| \leq \|g_{k+1}\|^2 + |\beta_k^{PRP}||d_k^t g_{k+1}|$. It follows from relation (3.1) that

$$\left|d_{k+1}^t g_{k+1}\right| \leq \|g_{k+1}\|^2 + 1.2\sigma \frac{\|g_k\|}{\|d_k\|} \|g_{k+1}\|^2 \leq (1+1.2\sigma\mu)\|g_{k+1}\|^2,$$

which means that $-\varpi\|g_{k+1}\|^2 \leq d_{k+1}^t g_{k+1} \leq \varpi\|g_{k+1}\|^2$, where $\varpi = (1+1.2\sigma\mu)$. This completes the proof. □

Lemma 4.2. *The sequence of steplengths* $\{\alpha_k\}_{k\in\mathbb{N}}$ *generated by the PRP-NLS algorithm under the new line search conditions* (2.1) *and* (2.2) *with* $\sigma \in \left(0, \frac{\mu-1}{1.2\mu^2}\right]$ *and* $1 < \mu < 2$ *satisfies*

$$\alpha_k \geq \frac{\sigma\|g_k\|^2/\|d_k\|^2 - 1}{L\|d_k\|^2} d_k^t g_k > 0, \forall k \in \mathbb{N}.$$

Proof. From Theorem 3.1, it results that $\sigma\frac{\|g_k\|^2}{\|d_k\|^2} < \frac{\mu-1}{1.2} < 1$. In view of condition (2.2), one sees that

$$0 < \left(\sigma\frac{\|g_k\|^2}{\|d_k\|^2} - 1\right) d_k^t g_k < d_k^t(g_{k+1} - g_k) \leq L\alpha_k\|d_k\|^2.$$

This completes the proof. □

Lemma 4.3. *Under Assumption 4.1, the sequences* $\{g_k\}_{k\in\mathbb{N}}$ *and* $\{d_k\}_{k\in\mathbb{N}}$ *produced by the PRP-NLS algorithm satisfy*

$$\sum_{k\geq 0} \frac{(g_k^t d_k)^2}{\|d_k\|^2} < +\infty. \tag{4.1}$$

Proof. Using condition (2.1), we have

$$f(x_k) - f(x_k + \alpha_k d_k) \geq -\delta\alpha_k g_k^t d_k \frac{\|g_k\|^2}{\|d_k\|^2} \geq \frac{\delta\alpha_k}{\varpi}\frac{(g_k^t d_k)^2}{\|d_k\|^2}.$$

Then $\frac{\delta\alpha_k}{\varpi}\frac{(g_k^t d_k)^2}{\|d_k\|^2} \leq f(x_k) - f(x_{k+1})$. Let $m = \min\{\alpha_k : k \in \mathbb{N}\}$. Under Assumption 4.1, by summing this inequality from $k = 0$ to infinity, we arrive at

$$\frac{\delta m}{\varpi}\sum_{k\geq 0}\frac{(g_k^t d_k)^2}{\|d_k\|^2} \leq \sum_{k\geq 0}\frac{\delta\alpha_k}{\varpi}\frac{(g_k^t d_k)^2}{\|d_k\|^2} < +\infty.$$

Thus (4.1) holds. □

Now, we are in a position to address the global convergence of the PRP-NLS algorithm.

Theorem 4.2. *Under the above assumptions, the PRP-NLS algorithm converges globally in the sense that* $\lim_{k\to+\infty}\|g_k\| = 0$.

Proof. Assume that $\lim_{k\to+\infty}\|g_k\|=0$ does not hold. Then, there exists a strictly positive value $r>0$ such that $\|g_k\|>r$ for all k in $\mathbb{N}$. Let $m=\min\{\alpha_k : k\in\mathbb{N}\}$ and $D=\max\{\|x-y\| : x,y\in\Omega\}$. From relation (1.1), we see that $\|d_k\|^2=\frac{\|x_{k+1}-x_k\|^2}{\alpha_k^2}\leq\frac{D^2}{m^2}$. Note that

$$d_{k+1}\leq\|g_{k+1}\|+\left|\beta_k^{PRP}\right|\|d_k\|\leq\Gamma+\left(\frac{1.2\Gamma^2}{r^2}\right)\frac{D}{m}=M.$$

Thus $\sum_{k\geq 0}\frac{1}{\|d_k\|^2}=+\infty$. From (3.6) and (4.1), we have

$$\xi^2r^4\sum_{k\geq 0}\frac{1}{\|d_k\|^2}\leq\sum_{k\geq 0}\frac{\xi^2\|g_k\|^4}{\|d_k\|^2}\leq\sum_{k\geq 0}\frac{(g_k^td_k)^2}{\|d_k\|^2}<+\infty.$$

It follows that $\sum_{k\geq 0}\frac{1}{\|d_k\|^2}<+\infty$, which yields a contradiction. This completes the proof. □

5. Computational Experiments

5.1. **Applications on typical test functions.** We present a series of computational performances concerning the PRP-NLS algorithm, applied on 270 test functions taken from CUTEr [9] and [1], as listed in Table 1, with dimensions ranging from 2 to 100000, as well as on restoring four images with different noise levels. All the codes are written and implemented in Matlab. In all experiments, the PRP-NLS algorithm is implemented with the setting parameters $\mu=1.6$, $\delta=10^{-4}$, and $\sigma=10^{-3}$.

To demonstrate the effectiveness of the suggested approach, we compared it with PRP [18] ($\theta=0.4$), PRP$^+$ [10] ($\delta=10^{-4}$ and $\sigma=10^{-3}$) and PRPMWWP [26] ($\delta=0.1\delta^*=0.05\delta_1=10^{-16}$ and $\sigma=0.9$). For this comparison, the same initial point is assigned for each test problem, and each implementation is considered successful if a point x_k, where $\|g(x_k)\|_\infty\leq 10^{-6}$ is reached within 2000 iterations, with CPU time less than 500 seconds; alternatively, the implementation is assigned as a failure.

In Figures 1-4, we compare the performance of the proposed method with PRP, PRP$^+$ and PRPMWWP methods by using the logarithmic performance profile of Dolan and Moré [7], relative to the number of iterations, function evaluations, gradient evaluations and CPU-time. For a solver s, we define the ratio

$$r_{\mathrm{P},s}=\frac{N_{\mathrm{P},s}}{\min\{N_{\mathrm{P},s}:s\in S\}},$$

where $N_{\mathrm{P},s}$ denotes either the number of iterations, the number of function (gradient) evaluations, or the CPU time required by the solver s to solve problem (P). If s does not solve Problem (P), the ratio $r_{\mathrm{P},s}$ is assigned a large number. The logarithmic performance profile for each solver s is defined as follows:

$$\rho_s(\tau)=\frac{\text{number of problems where }\log_2(r_{\mathrm{P},s})\leq\tau}{\text{total number of problems}}.$$

For each method, we plot the fraction $\rho_s(\tau)$ of problems for which the method has a number of iterations (resp. number of function (gradient) evaluations and CPU time) that is within a factor

Function	Dimension n	Function	Dimension n
Extended Maratos	500, 700, 1000,2000,4000, 9000, 9500, 60000, 10000, 15000	Arwhead	50, 60, 80, 100, 150, 200, 800, 1000, 5000
COSINE	10, 100 , 500, 1000	SINE	10, 100 , 500, 1000
ENGVAL1	100, 600, 800, 1000, 1500, 1600,1800, 10000	Diagonal 1	2,10, 100, 1000, 10000, 100000
Generalized Tridiagonal 1	2, 10, 20,300, 500, 700, 10000	FLETCHCR	2, 4
Extended White and Holst	1000, 2000, 3000, 4000, 5000, 6000	Diagonal 2	2, 4, 10, 800, 1000, 80000
Diagonal 7	500, 700, 1000, 1500, 2000, 7000, 8000	Extended Rosenbrock	10, 20,100 ,1200, 3000, 4000, 5000
Quadratic QF2	100, 200,1000,5000, 7000, 9000, 10000, 50000	Diagonal 8	100, 200, 400, 500, 1000, 1500, 2000
Extended Freudenstein and Roth	10, 100, 1000, 4000, 9000, 10000, 20000, 50000, 60000, 80000	Diagonal 3	2, 4, 6, 10, 50, 100, 200, 400, 700
DENSCHNF	10, 100, 10000, 25000, 30000 50000, 70000, 80000, 90000	Extended Himmelblau	4, 6,10, 9000, 10000
Perturbed Quadratic	2	POWER	2
QUARTC	2	Raydan 1	2
Generalized Rosenbrock	2, 50, 800, 1000	Perturbed quadratic diagonal	2
DENSCHNB	10, 90, 100, 2000, 3000, 4000, 5000, 6000, 7000, 9000	Raydan 2	1000, 4000, 50000,80000
HIMMELBG	2000, 3000, 6000, 30000, 50000, 80000	LIARWHD	10,50, 4000,5000, 5500, 10000, 20000, 80000
Extended quadratic exponential EP1	40000, 50000, 60000, 70000	Diagonal 5	100, 200, 700, 1000, 1500, 2000, 2200, 2500
Extended BD1	4, 800, 900, 2000, 3000, 5000 20000, 40000, 60000, 70000, 80000	Extended quadratic penalty QP1	4, 6, 8, 10, 50, 100, 700, 1000, 1500
Hager	2, 4,10,50, 80, 150, 300	NONSCOMP	2, 4, 1000, 5000, 70000
HIMMELLH	10, 50, 300, 500, 10000,50000, 60000, 80000, 10000	Quadratic QF1	5000, 6000, 8000, 9000, 20000, 50000, 70000, 80000
Extended quadratic penalty QP2	40, 60, 200	Diagonal 4	20000, 30000, 40000, 50000, 60000, 70000
DIXON3DQ	2, 4, 600	Extended PSC1	2, 4, 10, 100, 1000,10000
Almost Perturbed Quadratic	2, 4, 6	Diagonal 9	10, 30,50, 60, 70, 90
Extended Tridiagonal 1	6, 10, 20,80, 90, 100, 150, 300, 500, 700, 1000, 5000, 6000	NONDIA	10, 100,500,1000,5000,100000

TABLE 1. List of test functions.

τ. The curve that is shaped on the top corresponds to the code that solves the majority of the test problems within the given factor τ; for more details, see [7].

Figures 1-4 illustrate that the PRP-NLS method outperforms the others. Notably, it is faster for approximately 65% of the test problems and successfully solves around 96% of them, followed by the NPRP method with 94% of test problems. The PRPMWWP method solved around 93% of test problems, whereas the PRP method solved about 88% the test problems. These outcomes prove the competitiveness and rapid convergence of the PRP-NLS algorithm in the majority of the test problems.

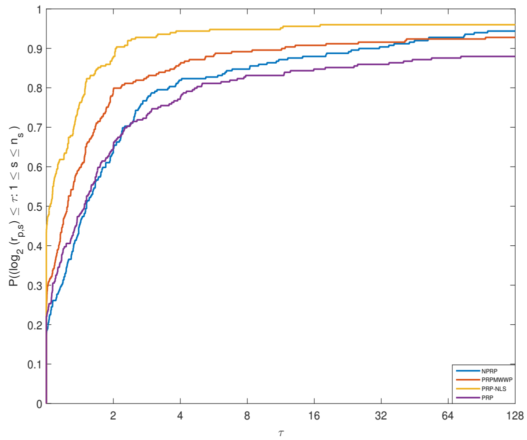

FIGURE 1. Performance profiles plot based on CPU time.

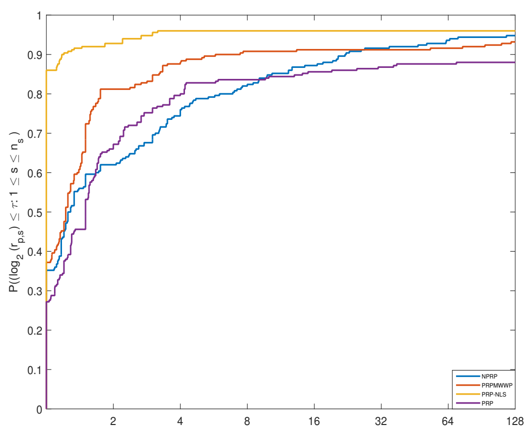

FIGURE 2. Performance profiles plot based on the number of iterations.

5.2. **Image restoration problems.** Image restoration problems aim to restore the original image which was corrupted by impulse noise. For this comparison, four test images (Man.png, Boat.png, Hill.jpg and Bridge.bmp) of size 512×512 are chosen to evaluate the effectiveness of the hPB algorithm against the same variants used in the previous comparisons. The image quality is assessed by two factors: the Peak Signal-to-Noise Ratio (PSNR) and its relative error (Err)

$$PSNR = 10 \log_{10} \frac{M \times N \times 255^2}{\sum_{i,j}(x^r_{i,j} - x^*_{i,j})^2}, \qquad Err = \frac{\|x^r - x^*\|}{\|x^*\|},$$

where M and N are the sizes of the image, $x^r_{i,j}$ represents the pixel values of the restored image and $x^*_{i,j}$ denotes the original pixel values. The setting parameters of the proponent algorithms are set similarly to the previous test, and each computation will stop if any of the following criteria are fulfilled

$$Iter > 300 \text{ or } \frac{|f(x_{k+1} - f(x_k)|}{|f(x_k)|} < 10^{-4}.$$

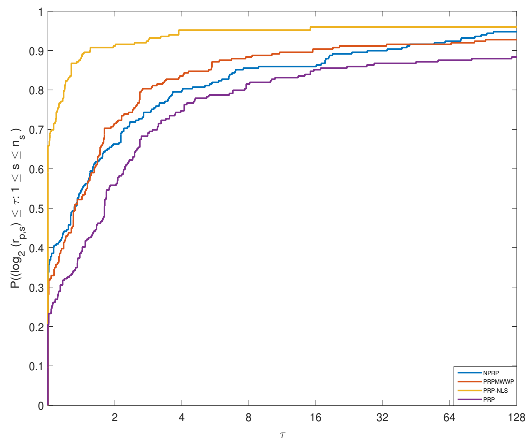

FIGURE 3. Performance profiles plot based on the number of function evaluations.

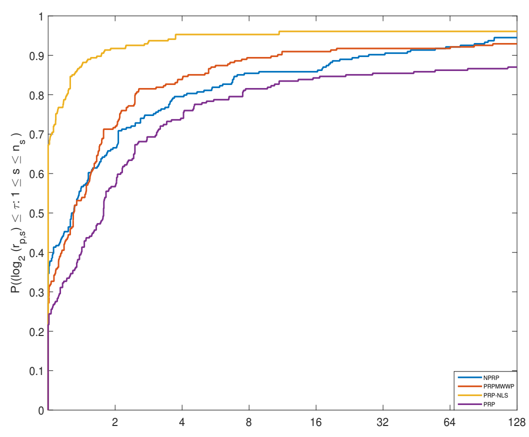

FIGURE 4. Performance profiles plot based on the number of gradient evaluations.

Figures 5, 6, and 7 display the restored images by impulse 30 %, 50%, and 70 % of noise. The performance of each algorithm is measured by the restored image quality, the elapsed time and the number of iterations. The numerical outcomes are reported in Tables 2 - 4. The algorithm with a high PSNR, minimal error, with less CPU time, is considered the best.

From the results in Tables 2 - 4 and Figures 5 - 7, one sees that the PRP-NLS algorithm delivers good performance. In fact, as illustrated in Table 2 and Figure 5, we can observe that the NPRP method fails to restore images with 30% of noise, whereas the other methods are successful with a PSNR greater than 25, and the hPB method has the highest PSNR value for the Man and Boat images. On the other hand, the visual outcomes of Figure 6 with 50% of noise show that the NPRP method also fails to remove the noise with a PSNR less than 25, whereas the PRPMWWP method fails to restore the image of Man, while the PRP and PRP-NLS methods succeed for restoring all the images and the bold values in Table 3 indicate the superiority of the PRP-NLS method for restoring all images. For 70% of noise, as shown in Figure 7 and Table 4, the NPRP method fails to restore the original images; while the other methods succeed

FIGURE 5. The restored images with 30% salt-and-pepper by PRP, NPRP, PRPMWWP and PRP-NLS.

Methods \ Images		Man	Boat	Hill	Bridge
PRP	Iter	11	11	16	14
	CPU	16.0896	14.6281	16.4851	15.5467
	PSNR	31.3374	**33.1674**	34.7344	28.5131
	Err	0.0564	**0.0406**	0.0381	0.0757
NPRP	Iter	**6**	**6**	**6**	**6**
	CPU	12.4714	**12.5510**	11.8639	**12.1049**
	PSNR	15.7089	17.5182	17.0148	16.2439
	Err	0.3410	0.2461	0.293465	0.3111
PRPMWWP	Iter	13	15	15	14
	CPU	17.8876	19.6420	16.0520	17.0935
	PSNR	**31.4483**	32.7617	**34.8471**	28.5141
	Err	**0.055693**	0.042564	**0.0376**	0.075770
PRP-NLS	Iter	8	8	9	8
	CPU	**12.3206**	13.9993	**11.6398**	12.4814
	PSNR	28.5141	31.4483	**34.8471**	**32.7617**
	Err	0.07577	0.055693	**0.0376**	**0.042564**

TABLE 2. The numerical outcomes of restoring images with 30% salt-and-pepper.

FIGURE 6. The restored images with 50% salt-and-pepper by PRP, NPRP, PRPMWWP and PRP-NLS.

Methods \ Images		Man	Boat	Hill	Bridge
PRP	Iter	20	17	21	24
	CPU	36.9955	24.7400	30.9204	38.2190
	PSNR	28.9228	30.8359	32.5124	26.4954
	Err	0.0744	0.0531	0.0492	0.0955
NPRP	Iter	6	**6**	12	**5**
	CPU	16.0684	18.4926	20.3538	16.2163
	PSNR	13.4675	15.1712	14.7113	14.1672
	Err	0.441405	0.322532	0.382587	0.395223
PRPMWWP	Iter	**5**	17	20	16
	CPU	16.5329	22.4427	29.8420	21.0229
	PSNR	15.3421	30.9165	32.4165	26.5201
	Err	0.355716	0.052639	0.0498	0.095324
PRP-NLS	Iter	14	15	**14**	15
	CPU	**15.5356**	**17.2738**	**15.325**	**15.2843**
	PSNR	**29.1751**	**31.1843**	**32.6828**	**26.7130**
	Err	**0.072353**	**0.051041**	**0.0483**	**0.093230**

TABLE 3. The numerical outcomes of restoring images with 50% salt-and-pepper.

FIGURE 7. The restored images with 70% salt-and-pepper by PRP, NPRP, PRPMWWP and PRP-NLS.

Methods \ Images		Man	Boat	Hill	Bridge
PRP	Iter	20	15	14	15
	CPU	34.7941	28.4139	32.8371	41.2126
	PSNR	26.1118	27.5034	25.6558	22.0517
	Err	0.1029	0.0779	0.1085	0.1594
NPRP	Iter	**6**	**6**	**6**	**6**
	CPU	**22.5660**	**20.0892**	**19.9322**	**19.4860**
	PSNR	11.3863	13.0485	12.5420	12.1776
	Err	0.560914	0.411816	0.491131	0.496963
PRPMWWP	Iter	29	24	16	21
	CPU	30.3015	35.5985	29.1123	35.9517
	PSNR	26.1898	28.2480	29.3224	24.1335
	Err	0.102028	0.071570	0.0711	0.125468
PRP-NLS	Iter	27	20	18	22
	CUP	28.8349	25.3926	27.1979	25.1883
	PNSR	**26.3222**	**28.2927**	**29.8827**	**24.5192**
	Err	**0.100484**	**0.071202**	**0.0667**	**0.120017**

TABLE 4. The numerical outcomes of restoring images with 70% salt-and-pepper.

in restoring the images of Man, Boat and Hill, where the highest PSNR value corresponds to the PRP-NLS method. Overall, the numerical and visual outcomes of removing $30\%, 50\%$, and 70% of noise show a satisfactory performance of the PRP-NLS algorithm. Notably, the bold values in Tables 2 - 4 highlight the efficiency of the proposed algorithm, as it achieves higher PSNR values and takes a short time to restore the majority of the test images.

6. Conclusion

This paper presents an accelerated version of the PRP conjugate gradient method by introducing a novel inexact line search technique for solving nonlinear unconstrained optimization problems. The existence of a step length that satisfies the proposed line search conditions was established. The convergence properties of the proposed PRP-NLS approach were analyzed under the new line search conditions, and the global convergence was obtained under mild assumptions. To evaluate the efficiency and robustness of the suggested PRP-NLS method in practical computations, it was compared with three similar PRP variants: PRP, PRP^+, and PRPMWWP. The comparison was conducted by using four performance criteria: the number of iterations, CPU time, the number of function evaluations, and the number of gradient evaluations. It was reported that the proposed method performs better than the others. Furthermore, based on some restoring image problems, the PRP-NLS method was successfully applied for restoring original images with higher PSNR values. These preliminary results confirm the robustness and competitiveness of the proposed approach.

References

[1] N. Andrei, An unconstrained optimization test functions, Adv. Modeling Optim. 10 (2008), 147-161.

[2] A.M. Awwal, K. Ahmed, P. Sukprasert, K. Khammahawong, A spectral class of Dai-Kou-type methods with applications to signal processing, J. Nonlinear Funct. Anal. 2024 (2024), 32.

[3] Y. Bai, J. Chen, L. Tang, T. Zhang, Convergence of a new nonmonotone memory gradient method for unconstrained multiobjective optimization via robust approach, J. Nonlinear Var. Anal. 8 (2024), 625-639.

[4] Y.H. Dai, Analyses of Nonlinear Conjugate Gradient Methods, Ph. D. thesis, Institute of Computational Mathematics and Scientific/Engineering Computing, Chinese Academy of Sciences, 1997.

[5] Y.H. Dai, Y. Yuan, An efficient hybrid conjugate gradient method for unconstrained optimization, Ann. Oper. Res. 103 (2001), 33-47.

[6] T. Diphofu, P. Kaelo, An efficient conjugate gradient method based on the conjugacy condition with an application in motion control, Iranian J. Sci. 49 (2025), 1327–1334.

[7] E.D. Dolan, J.J. Moré, Benchmarking optimization software with performance profiles, Math. Program. 91 (2002), 201-213.

[8] R. Fletcher, Practical Method of Optimization, 2nd ed., Wiley, New York, 1997.

[9] N.I. Gould, D. Orban, P. L. Toint, CUTEr and SifDec: A constrained and unconstrained testing environment, revisited, ACM Trans. Math. Softw. 29 (2003), 373-394.

[10] J. Gilbert, J. Nocedal, Global convergence properties of conjugate gradient methods for optimization, SIAM J. Optim. 2 (1992), 21-42.

[11] R. Glowinski, D.A. León-Velasco, L.H. Juérez-Valencia, J.J. Conde-Mones, J.J. Oliveros-Oliveros, A boundary operator approach for the solution of a biharmonic problem from inverse source problems, Commun. Optim. Theory 2023 (2023), 36.

[12] M.R. Hestenes, E. Stiefel, Method of conjugate gradient for solving linear equations, J. Res. Nat. Bureau Standards, 49 (1952), 409-436.

[13] Y. Liu, C. Storey, Efficient generalized conjugate gradient algorithms. Part 1: Theory, J. Optim. Theory Appl. 69 (1992), 129-137.

[14] A. Maiza, R. Ziadi, M. A. Saleh, A. Z. Almaymuni, An improved conjugate gradient algorithm by adapting a new line search technique, Electron. Res. Archive, 33 (2025), 2148-2171.

[15] A. Maiza, R. Ziadi, M. A. Saleh, A. Z. Almaymuni, A combination of two conjugate gradient methods under a new line search with its application in image restoration problems, Int. J. Appl. Math. Comput. Sci. 35 (2025), 267-280.

[16] M.J. Powell, Nonconvex minimization calculations and the conjugate gradient method. In: D.F. Griffiths, (eds) Numerical Analysis. Lecture Notes in Mathematics, vol 1066. Springer, Berlin, Heidelberg.

[17] E. Polak, G. Ribière, Note sur la convergence de méthodes des directions conjuguées, Revue Francaise d'informatique et Recherche Opérationelle, 16 (1969), 35-43.

[18] B.T. Polyak, The conjugate gradient method in extreme problems, Comput. Math. Math. Phys. 9 (1969), 94-112.

[19] C. Souli, R. Ziadi, A. Bencherif-Madani, H. M. Khudhur, A hybrid CG algorithm for nonlinear unconstrained optimization with application in image restoration, J. Math. Model. 2 (2024), 301-317.

[20] C. Souli, R. Ziadi, I. Lakhdari, A. Leulmi, An efficient hybrid conjugate gradient method for unconstrained optimization and image restoration problems, Iranian J. Numer. Anal. Optim. 15 (2025), 99-123.

[21] Z. Wei, S. Yao, L. Liu, The convergence properties of some new conjugate gradient methods, Appl. Math. Comput. 183 (2006), 1341-1350.

[22] O.O.O. Yousif, M.A.Y. Mohammed, M.A. Saleh, M.K. Elbashir, A criterion for the global convergence of conjugate gradient methods under strong Wolfe line search, J. King Saud Univ. Sci. 34 (2022), 1-7.

[23] O.O.O. Yousif, R. Ziadi, M.A. Saleh, A.Z. Almaymuni, An improved version of Polak-Ribière-Polyak conjugate gradient method with its applications in neural networks training, Electron. Res. Archive, 33 (2025), 4799-4815.

[24] G. Yu, L. Guan, Z. Wei, Globally convergent Polak–Ribière–Polyak conjugate gradient methods under a modified Wolfe line search, Appl. Math. Comput. 215 (2009), 3082-3090.

[25] G. Yuan, Z. Wei, Y. Yang, The global convergence of the Polak–Ribière–Polyak conjugate gradient algorithm under inexact line search for nonconvex functions, J. Comput. Appl. Math. 362 (2019), 262-275.

[26] G. Yuan, L. Guan, Z. Wang, The PRP conjugate gradient algorithm with a modified WWP line search and its application in the image restoration problems, Appl. Math. Comput. 152 (2020), 1-11.

[27] W. Zhou, D.H. Li, On the convergence properties of the unmodified PRP method with a non-descent line search, Optim. Meth. Softw. 2 (2014), 484-496.

[28] R. Ziadi, R. Ellaia, A. Bencherif-Madani, Global optimization through a stochastic perturbation of the Polak-Ribière conjugate gradient method, J. Comput. Appl. Math. 317 (2017), 672-684.

[29] R. Ziadi, A. Bencherif-Madani, A perturbed quasi-Newton algorithm for bound-constrained global optimization, J. Comput. Math. 43 (2025), 143-173.